Cerebral Cortex August 2011;21:1818–1826
doi:10.1093/cercor/bhq257
Advance Access publication January 10, 2011

Specificity of Synaptic Connectivity between Layer 1 Inhibitory Interneurons and Layer 2/3 Pyramidal Neurons in the Rat Neocortex

Christian Wozny[1] and Stephen R. Williams[1,2]

[1]MRC Laboratory of Molecular Biology, Cambridge CB2 0QH, UK and [2]The Queensland Brain Institute, St Lucia, QLD 4072, Australia

Address correspondence to Stephen R. Williams and Christian Wozny. Email: srw@uq.edu.au and cwozny@mrc-lmb.cam.ac.uk.

Understanding the structure and function of the neocortical microcircuit requires a description of the synaptic connectivity between identified neuronal populations. Here, we investigate the electrophysiological properties of layer 1 (L1) neurons of the rat somatosensory neocortex (postnatal day 24–36) and their synaptic connectivity with supragranular pyramidal neurons. The active and passive properties of visually identified L1 neurons ($n = 266$) suggested division into 4 groups according to the Petilla classification scheme with characteristics of neurogliaform cells (NGFCs) ($n = 72$), classical-accommodating ($n = 137$), fast-spiking ($n = 23$), and burst-spiking neurons ($n = 34$). Anatomical reconstructions of L1 neurons supported the existence of 4 major neuronal groups. Multiparameter unsupervised cluster analysis confirmed the existence of 4 groups, revealing a high degree of similarity with the Petilla scheme. Simultaneous recordings between synaptically connected L1 neurons and L2/3 pyramidal neurons ($n = 384$) demonstrated neuronal class specificity in both excitatory and inhibitory connectivity and the properties of synaptic potentials. Notably, all groups of L1 neurons received monosynaptic excitatory input from L2/3 pyramidal neurons ($n = 33$), with the exception of NGFCs ($n = 68$ pairs tested). In contrast, NGFCs strongly inhibited L2/3 pyramidal neurons ($n = 12$ out 27 pairs tested). These data reveal a high specificity of excitatory and inhibitory connections in the superficial layers of the neocortex.

Keywords: cortical column, GABAergic interneuron, layer 1, layer 2/3, neurogliaform cell, synaptic connectivity, target-cell specificity

Introduction

The neocortex is a 6-layered structure which is functionally organized into columns (Mountcastle 1997). Understanding the wiring diagram of a cortical column has received much attention in recent years (Douglas and Martin 2004). The excitatory synaptic circuitry of the cortical column has been well described (Lubke and Feldmeyer 2007; Schubert et al. 2007). The neocortex, however, is not only composed of excitatory neurons but also γ-aminobutyric acid (GABA)ergic inhibitory interneurons, which make up ~20% of the neocortical neuronal population. Inhibitory interneurons can be classified by morphological, electrophysiological, neurochemical features (Ascoli et al. 2008), and their transcriptional regulation during development (Butt et al. 2007; Batista-Brito and Fishell 2009). The distribution of interneuron classes, however, differs across neocortical layers (Markram et al. 2004; Ascoli et al. 2008).

Layer 1 (L1) of the neocortex is a cell-sparse synaptic and axon dense zone. In contrast to other neocortical layers, L1 is composed of more than 90% of GABAergic neurons (Winer and Larue 1989; Prieto et al. 1994). In the primary somatosensory cortex, whisker-evoked sensory information is rapidly relayed to L1 neurons (Zhu Y and Zhu JJ 2004), which, in turn, act to powerfully inhibit sensory-evoked responses in L2/3 (Shlosberg et al. 2006). Surprisingly, the interneuronal composition and synaptic connectivity of L1 neurons have not been explored in detail (Hestrin and Armstrong 1996; Zhou and Hablitz 1996a, 1996b; Chu et al. 2003; Zhu Y and Zhu JJ 2004). Layer 1 constitutes an important site of integration in the neocortical column as it contains a dense plexus of the apical dendrites of layer 2/3 and layer 5 pyramidal neurons and axons originating from a variety of cortical areas (Cauller et al. 1998; Mitchell and Cauller 2001; Petreanu et al. 2009) and the thalamus (Rubio-Garrido et al. 2009). Long-range intracortical excitatory axons, conveyed in L1, synapse with both the apical dendrites of pyramidal neurons (Petreanu et al. 2009) and local GABAergic interneurons (Anderson and Martin 2006). Thus, L1 inhibitory interneurons are ideally placed to control dendritic synaptic integration in pyramidal neurons (Williams and Stuart 2002; Waters et al. 2003; Williams 2004; Larkum et al. 2009).

In this study, we have characterized the electrophysiological properties of L1 neurons of the rat neocortex and investigated the synaptic connectivity between L1 inhibitory interneurons and L2/3 pyramidal neurons. Our results provide new insights into the wiring diagram of the superficial layers of the neocortical column.

Materials and Methods

Slices and Recordings

Wistar rats (P24 to P36) were decapitated under deep isoflurane anesthesia following UK Home office and institutional guidelines. Brains were quickly removed and placed into ice-cold solution containing (mM): NaCl 125, $NaHCO_3$ 25, KCl 3, NaH_2PO4 1.25, $CaCl_2$ 1, $MgCl_2$ 6, sodium pyruvate 3, and glucose 25, oxygenated at 95% O_2 and 5% CO_2. After cutting coronal sections (300–350 μm) of the somatosensory cortex (slices were collected corresponding to the coordinates of Bregma ca. –3.8 mm to Bregma ca. –1.8 mm Paxinos and Watson 1998), slices were incubated at 34 °C for 30 min and then stored at room temperature. For recordings, a single brain slice was placed in a chamber perfused with a solution of composition (mM): NaCl 125, $NaHCO_3$ 25, KCl 3, NaH_2PO4 1.25, $CaCl_2$ 2, $MgCl_2$ 1, sodium pyruvate 3, and glucose 25 at 34–36 °C. Double and triple whole-cell recordings from the somata of layer 1 (L1) and layer 2/3 (L2/3) somatosensory neocortical neurons were made with identical current clamp amplifiers (BVC 700A; Dagan). The L1–L2 border was defined by the abrupt change in the density of neurons visualized under infrared differential interference contrast video microscopy. Pipettes were filled with a solution containing (mM): potassium gluconate 135, NaCl 7, Hepes 10, Na_2-ATP 2, Na-GTP 0.3, $MgCl_2$ 2, and occasionally with Alexa Fluor 568 0.01–0.04 (Molecular Probes) for visualization after recording; pH was adjusted to 7.2–7.3 with KOH.

Intrinsic Properties of L1 and L2/3 Neurons

The action potential (AP) firing pattern of neurons was investigated by the injection of a series of 600 ms positive current steps through the

recording pipette (100 pA steps up to a maximum of 1 nA). Input resistance (R_{in}) was calculated from the steady-state voltage change evoked by the injection of a 100 pA negative current step. Resting membrane potential (RMP) was measured at the beginning of each recording and was not corrected for the liquid junction potential. The accommodation of a neuron's AP firing frequency was assessed by calculating an accommodation index, which is defined as the ratio of the first and last interspike interval at threshold for repetitive AP firing. We did not estimate the rheobase of neurons as we injected current through the patch pipette in 100 pA steps and therefore the accommodation index was calculated at near-threshold voltages.

Cluster Analysis

To cluster L1 neurons into groups, unsupervised clustering was performed using Ward's method (WinSTAT) (for details, see Ward 1963; Cauli et al. 2000). The results of the cluster analysis were compared with the classification of neurons according to the Petilla terminology (see Results; Ascoli et al. 2008).

Synaptic Connectivity

Excitatory and inhibitory synaptic transmission was examined between simultaneously recorded L2/3 pyramidal neurons and L1 neurons. Synaptic connectivity was tested for by the repeated generation of a pair of APs (evoked by 2 ms test pulses; 0.5–5 nA; separated by 50 ms; delivered at 0.33 Hz). If neurons were not synaptically connected, one of the recording electrodes was withdrawn and either a new pyramidal neuron or interneuron recorded. Voltage and current signals were low-pass filtered at 10 kHz and acquired at 25–50 kHz using an ITC-18 interface (HEKA) controlled by an Apple computer. Data were analyzed and curve fitting performed using Axograph X. Unitary postsynaptic potential (uPSP) onset time, rise time, and half-width was measured from either single episodes or from averages (usually 50 responses). Onset was determined at 5% of peak response, rise time was measured as the time to reach between 10 and 90% of the maximal amplitude of the uPSP, and the decay time constants were determined by fitting the decay with a single exponential function. To accurately measure the amplitude of the second uPSP following a paired-pulse stimulus, the decay of first uPSP was fitted with an exponential function, which was subsequently subtracted from the trace. The amplitude of the second uPSP was measured over a window centered around peak amplitude relative to the subtracted trace. Statistical analysis was performed with Student's *t*-test (Excel, Microsoft), chi-squared test, Fisher's Exact test, or with an analysis of variance (ANOVA) test (all Sigma-Plot).

Reconstructions

Neurons were filled with biocytin (0.5%, added to the pipette recording solution) and slices fixed overnight in 4% paraformaldehyde dissolved in 0.1 M sodium phosphate-buffered saline (PBS, pH 7.4). Subsequently, slices were incubated for 12–18 h in PBS supplemented with 0.5–2% Triton X-100 and 0.2% streptavidin, Alexa Fluor 488 conjugate (Invitrogen) at 4–6 °C. After washing with PBS, slices were mounted on slides, covered with Vectashield and coverslipped (Vector Laboratories). Confocal images were taken with Zeiss 510 or Zeiss 710 confocal microscope, respectively. Neuronal morphology was reconstructed from confocal image stacks using Neurolucida software (MBF Bioscience).

Results

Electrophysiological Properties of Layer 1 Neurons

We recorded from 271 layer 1 (L1) neurons located at least 20 μm from the L1–L2 border, selected irrespective of their morphology under infrared differential interference contrast video microscopy, using whole-cell current clamp techniques. Despite this selection criteria, 5 of 271 neurons had electrophysiological properties similar to those of simultaneously recorded L2/3 pyramidal neurons (n = 384; low input resistance and prominent rectification of the voltage–current relationship, see Supplementary Fig. 1). We first classified the remaining 266 L1 neurons according to their repetitive AP firing patterns in response to suprathreshold injection of positive current steps (Fig. 1). We observed key differences between groups of neurons in the initial AP firing frequency, the half-width of the first AP, and accommodation index (Fig. 1; see Materials and Methods). According to the Petilla classification scheme (Ascoli et al. 2008), we observed regular- (n = 209), fast- (n = 23), and burst-spiking (BS) neurons (n = 34). Regular-spiking behavior was observed in a group of neurons termed classical-accommodating neurons (c-AC, n = 137) and in a group resembling neurogliaform cells (NGFCs, n = 72) (Tamas et al. 2003; Olah et al. 2007; Szabadics et al. 2007). Most of the fast-spiking (FS) neurons were observed at the L1-L2 boarder (see anatomical features below). BS neurons showed high initial (burst) frequency (Fig. 1*A*,*B*). We divided neuronal classes according to their accommodation index (see Materials and Methods), which separated c-AC from NGFC cells (Fig. 1*C*) and the half-width of the first AP, which was narrowest in FS cells (Fig. 1*D*, Table 1). These quantitative measures allowed the clear division of L1 neurons into 4 groups.

When we examined the passive properties of neurons grouped by their AP properties, we found that the input resistance (R_{in}) and RMP of each group possessed surprisingly narrow boundaries. c-AC cells had an average input resistance of 166 ± 5 MΩ (n = 137), NGFC cells 107 ± 3 MΩ (n = 72), FS cells 87 ± 7 MΩ (n = 23), and BS cells 201 ± 15 MΩ (n = 34) (ANOVA on ranks, Kruskal–Wallis followed by a Dunn's test:

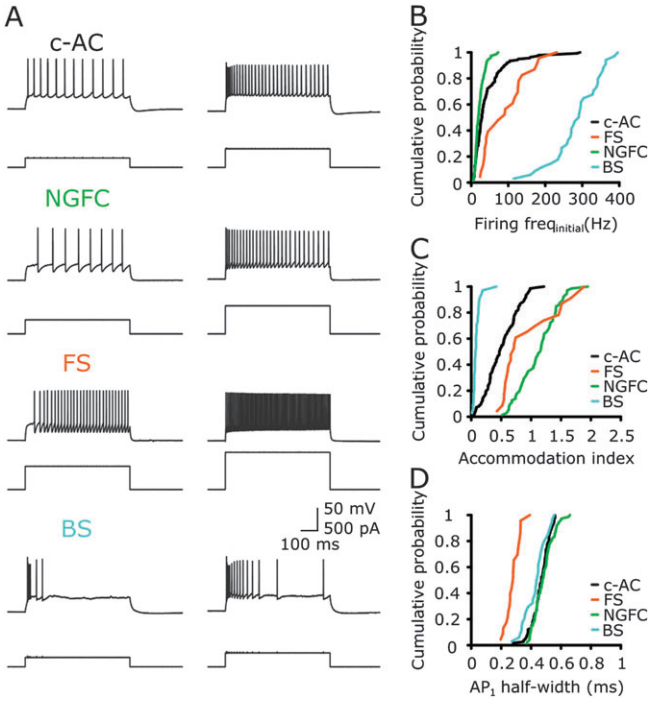

Figure 1. Electrophysiological characterization of L1 neurons. (*A*) Representative AP firing patterns of L1 neurons (upper traces), generated in response to the injection of positive current steps (lower traces). L1 neurons were classified according to their firing properties with respect to the Petilla classification scheme: c-AC, NGFCs, FS, and BS neurons. (*B–D*) The cumulative probability distributions of initial firing frequency, accommodation index, and half-width of the first AP_1 are shown for each type of L1 neurons (color code: c-AC: black, n = 137; NGFC: green, n = 72; FS: orange, n = 23; BS: blue, n = 34).

Table 1
Intrinsic properties of L1 neurons

	RMP (mV)	R_{in} (MΩ)	Firing $Freq_{initial}$ (Hz)	AP_1 half-width (ms)	Accommodation index ($t(AP_2 - AP_1)/t(AP_{n-1} - AP_n)$)
Petilla					
NGFC (72)	−73.4 ± 0.5	107 ± 3	23.0 ± 1.6	0.48 ± 0.01	1.12 ± 0.04
FS (23)	−72.0 ± 1.1	87 ± 7	93.0 ± 12.5	0.28 ± 0.01	0.93 ± 0.1
c-AC (137)	67.3 ± 0.4	166 ± 5	44.5 ± 4.2	0.5 ± 0.01	0.50 ± 0.02
BS (34)	−69.2 ± 0.9	201 ± 15	285.9 ± 11.3	0.43 ± 0.01	0.09 ± 0.01
Clustering					
Cluster 1 (81) (81% NGFC)	−74.0 ± 0.4 (−74.1 ± 0.5)	108 ± 3 (106 ± 3)	23.8 ± 2.3 (21.7 ± 1.5)	0.49 ± 0.1 (0.48 ± 0.01)	1.06 ± 0.04 (1.14 ± 0.04)
Cluster 2 (24) (96% FS)	−72.0 ± 1.1 (−72.0 ± 1.1)	88 ± 7 (87 ± 8)	92.8 ± 12.0 (93.0 ± 12.5)	0.28 ± 0.01 (0.28 ± 0.01)	0.91 ± 0.1 (0.93 ± 0.1)
Cluster 3 (125) (94% c-AC)	−66.2 ± 0.4 (−66.4 ± 0.4)	167 ± 4 (169 ± 4)	41.2 ± 3.2 (39.7 ± 3.2)	0.50 ± 0.01 (0.50 ± 0.01)	0.51 ± 0.02 (0.49 ± 0.02)
Cluster 4 (36) (89% BS)	−69.7 ± 0.7 (−69.8 ± 0.8)	209 ± 17 (202 ± 16)	286.3 ± 11.3 (295.2 ± 9.9)	0.43 ± 0.01 (0.43 ± 0.01)	0.09 ± 0.01 (0.08 ± 0.01)

Petilla: The active and passive properties of L1 neurons grouped according to the Petilla classification scheme (c-AC, NGFC, FS, and BS). Number of neurons are given in brackets. Clustering: unsupervised clustering (hierarchical clustering using Ward's method) was performed and a cut off criteria was determined to reveal 4 clusters. Number of neurons in each cluster are given in brackets. The primary composition of neurons in each cluster when identified by the Petilla classification scheme are indicated: 81% of neurons in cluster 1 were NGFCs, 96% of neurons in cluster 2 FS neurons, 94% of neurons in cluster 3 c-AC neurons, and 89% of neurons in cluster 4 BS neurons. The average values for the active and passive properties for the primary composition of neurons in each cluster. All values are given as mean ± standard error of the mean.

$P < 0.05$ for all pairwise multiple comparisons, except for c-AC vs. BS and NGFC vs. FS). Seventy-nine percent of NGFC cells and 83% of FS cells had R_{in} of less than 130 MΩ, whereas 80% of either c-AC cells and 82% BS cells had R_{in} of more than 130 MΩ (Fig. 2*A*,*B*). The RMP of 81% of NGFC cells and 78% of FS cells had an RMP depolarized to −70 mV, whereas the RMP of 23% of c-AC cells were hyperpolarized to −70 mV (Fig. 2*C*). BS cells showed a heterogeneous RMP distribution (Fig. 2*C*). These results are summarized in Table 1 (RMP: ANOVA on ranks, Kruskal–Wallis followed by a Dunn's test: $P < 0.05$ for all pairwise multiple comparisons, except for c-AC vs. BS and NGFC vs. FS).

Anatomical Features of L1 Neurons

Neurons were regularly filled with biocytin and subsequently processed for morphological reconstruction ($n = 71$). In 40 of 71 neurons, the axonal arborization was sufficiently stained for further analysis. Typical reconstructions for each neuronal type are shown in Figure 3. The neurites of 13 of 21 c-AC neurons were confined to L1 (62%, Fig. 3*A*), 5 had 1 or 2 axonal branches descending to deeper layers (Supplementary Fig. 2*B*), and a further 2 neurons had more than 2 descending axonal branches. One c-AC neuron showed a divergent morphology. All successfully reconstructed NGFCs ($n = 12$) had characteristic anatomical features, typified by a large and dense axonal field and short dendrites (Fig. 4*B*) (Tamas et al. 2003; Olah et al. 2007; Szabadics et al. 2007). The axonal arborization of 5 NGFCs was confined to layer 1, while 7 neurons had multiple descending axons (Fig. 3*B*). Located close to the L1-L2/3 boarder 5 FS cells were reconstructed; 1 had multipolar dendrites and an axonal arbor in deep L1 and superficial part of L2 (Fig. 3*C*) and 4 were found to be chandelier cells, which had the well-described feature of several hundreds of vertically oriented axonal segments targeting the axon initial segments of pyramidal neurons (Supplementary Fig. 3) (Somogyi 1977; Howard et al. 2005). The active properties of FS neurons that were anatomically identified as chandelier cells had unique electrophysiological properties, exhibiting a left-shifted relationship between injected current and AP firing frequency (Supplementary Fig. 4*A*) and transient stuttering AP firing upon threshold current injection (Supplementary Fig. 4*C*1,4*C*2), which was not be observed in other FS cells (Supplementary Fig. 4*B*) (Woodruff et al. 2009). Two BS neurons were also found to have multipolar dendrites and axonal branches ending in layer 1 and layer 2/3 (Fig. 3*D*).

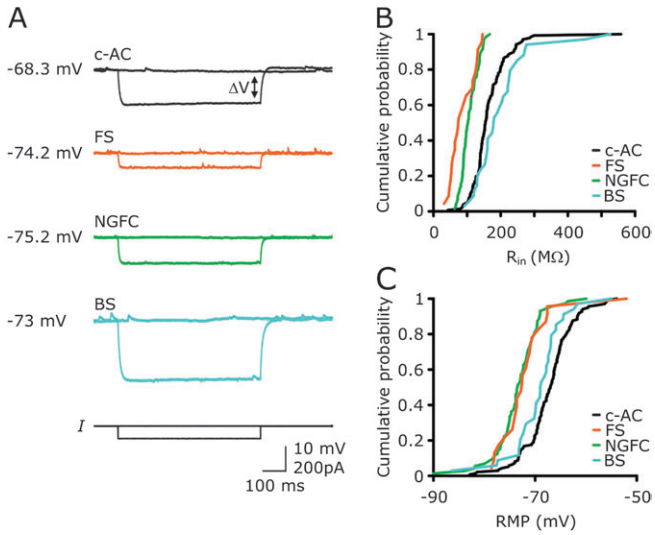

Figure 2. Passive properties of c-AC, NGFCs, FS, and BS neurons. (*A*) Example traces of voltage responses (upper traces) evoked the injection of a 100 pA negative current step (lower trace) in each cell type. The RMP is indicated. (*B*) Distribution of apparent input resistance (R_{in}, measured at steady state, indicated as ΔV by the arrow in A) and (*C*) RMP of each cell type. Data are presented as cumulative probability plots (color code: c-AC: black, $n = 137$; NGFC: green, $n = 72$; FS: orange, $n = 23$; BS: blue, $n = 34$).

Unsupervised Clustering

We used unsupervised cluster analysis (using Ward's method) to independently classify L1 neurons. Five electrophysiological parameters were used in this analysis: initial firing rate, accommodation index, half-width of the first AP, R_{in}, and RMP. Figure 4*A* shows the tree diagram of clusters based on these parameters; when a threshold of 4 clusters was selected, we found that neuronal grouping was similar to the Petilla classification. The first cluster was composed of 66 NGFCs and 15 c-AC neurons. The second cluster contained 96% FS cells. The majority of L1 neurons were grouped in the third cluster: 117 c-AC neurons, 6 NGFCs, and 2 BS neurons. The fourth cluster was composed of 89% BS cells (Fig. 4). Thus,

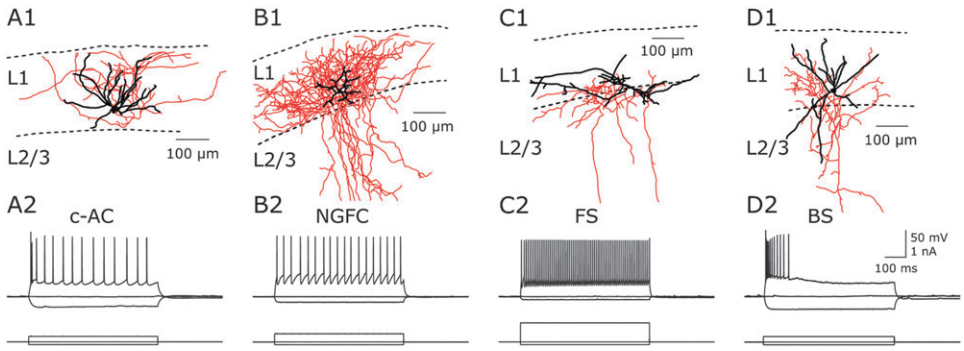

Figure 3. Anatomical reconstructions of L1 neurons. (*A1*) Typical example of a c-AC neuron with neurites confined to L1, dendrites are shown in black, and axon in red. (*B1*) Representative example of an NGFC with anatomical characteristics of a large and dense axonal field and short dendrites. (*C1*) Reconstruction of an FS neuron located at the boarder of L1 and L2. (*D1*) Example of a BS neuron with multipolar dendritic and axonal arbor in L1 and L2/3. Laminar borders are indicated with dashed lines. (*A2–D2*) AP firing pattern of the reconstructed L1 neurons (upper traces) in response to current injection (lower traces).

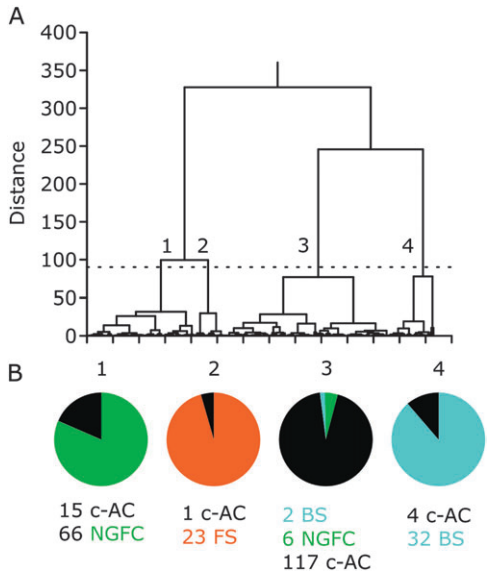

Figure 4. Cluster analysis of the electrophysiological properties of L1 neurons. (*A*) Tree diagram obtained using Ward's method. Five parameters were used to cluster neurons: initial firing rate, accommodation index, half-width of the first AP, R_{in}, and RMP. The dashed line indicates the chosen cut off. Clusters are numbered from 1 to 4. (*B*) Pie chart illustrating the composition of each cluster with reference to the Petilla classification scheme. The first cluster comprises 81 neurons, 66 of which had been classified as NGFCs and 15 as c-ACs. The second cluster is composed of 24 neurons, 23 FS and 1 c-AC neurons, the third cluster of 117 c-AC, 6 NGFCs, 2 BS neurons, and the fourth cluster of 32 BS and 4 c-AC neurons (color code: c-AC: black, NGFC: green, FS: orange, BS: blue).

unsupervised cluster analysis confirmed the presence of 4 groups: NGFCs, FS, c-AC, and BS neurons. For all subsequent analysis, we excluded all neurons that did not unequivocally belong to the same group using both classification schemes. We therefore excluded 8% of NGFC, 15% of c-AC, and 6% of BS cells from our initial groups based on the Petilla scheme (Fig. 4*B*). The electrophysiological properties of neurons grouped according to the Petilla classification scheme and following refinement based on cluster analysis are summarized in Table 1.

Synaptic Interaction between L2/3 Pyramidal Neurons and L1 Interneurons

Next, we investigated how efficiently L2/3 pyramidal neurons excited L1 interneurons (vertical distance up to ~250 µm, horizontal distance less than 100 µm between L2/3 Pyr–L1 pairs). The properties of unitary excitatory postsynaptic potentials (uEPSPs) were found to be dependent on the identity of the postsynaptic neuron. We analyzed the latency, the rise time, the amplitude, and the half-width of the uEPSPs (Fig. 5). L2/3-FS uEPSPs had a latency of 1.4 ± 0.2 ms, a rise time of 1.1 ± 0.1 ms, amplitude of 1.1 ± 0.3 mV, a half-width of 5.7 ± 0.7 ms, and a decay time constant of 7.4 ± 1.1 ms (n = 7, Supplementary Fig. 5). L2/3-c-AC uEPSPs had a latency of 1.8 ± 0.1 ms (P = 0.06), a slower mean rise time of 2.2 ± 0.2 ms (P < 0.001), a similar average mean amplitude of 1.1 ± 0.2 mV, a longer half-width of 17.2 ± 1.2 ms (P < 0.001), and a greater decay time constant of 25.0 ± 4.2 (P < 0.001, n = 21, Supplementary Fig. 5). L2/3-BS connections had a latency similar to the L2/3-c-AC and L2/3-FS connections (1.4 ± 0.3 ms, P > 0.05), a rise time of 2.4 ± 0.1 ms, an amplitude of 1.1 ± 0.4 mV, a half-width of 14.5 ± 2.0 ms, and a decay time constant of 21.5 ± 3.5 ms (n = 5, Supplementary Fig. 5). The latter properties were not significantly different from the properties of L2/3-c-AC connections but distinct from L2/3-FS connections (rise time, P < 0.001; half-width, P < 0.05; decay time constant, P < 0.05). The connectivity probability between identified L2/3 pyramidal neurons and L1 interneurons was calculated as the ratio of the number of synaptic connected neurons to the number of connections tested (Fig. 5). Surprisingly, none of the NGFCs tested received excitatory input from L2/3 pyramidal neurons (68 connections tested), whereas L2/3 pyramidal neurons had a high probability of connectivity with FS cells (0.35, 7/20 connections tested, significantly different from L2/3 Pyr-NGFC ratio, P < 0.001, Fisher's Exact test, and from L2/3 Pyr-c-AC and L2/3 Pyr-BS ratio, P < 0.05, chi-squared test). c-AC and BS neurons were found to receive excitatory input from L2/3 pyramidal neurons with a probability of 0.16 (21/134) and 0.12 (5/42), respectively (both significantly different from L2/3-NGFC ratio, Fisher's Exact test, P < 0.05). These data indicate that L2/3 pyramidal neurons target L1 interneurons in a class-specific manner.

We next investigated if the use-dependent properties (use-dependent depression or facilitation) of the excitatory synaptic input to classes of L1 interneurons were target cell dependent. To test this, we evoked 2 APs in L2/3 pyramidal neurons at an interval of 50 ms. Notably, use-dependent plasticity of L2/3 Pyr-FS and L2/3 Pyr-c-AC uEPSPs was distinct, L2/3 Pyr-FS uEPSPs

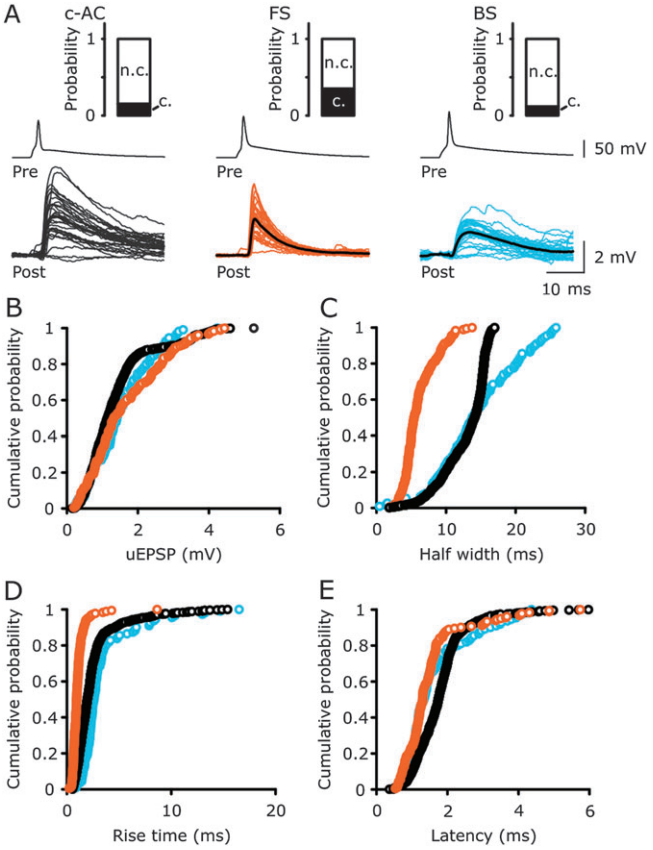

Figure 5. Properties of unitary EPSPs recorded in different types of L1 interneurons evoked by single AP firing in L2/3 pyramidal neurons. (*A*) Overlain traces of uEPSPs recorded from a c-AC (black), FS (orange), and BS(green) neuron. Average uEPSPs are shown as thick black traces. Pre, presynaptic L2/3 pyramidal neuron, post, postsynaptic L1 neuron. Inset shows probability of connectivity for each type of L1 neuron. (*B–E*) Distributions of the peak amplitude (*B*), half-width (*C*), 10–90% rise time (*D*), and latency (*E*) of uEPSPs recorded from 21 c-AC (n = 792 uEPSPs, black), 7 FS (n = 182 uEPSPs, orange), and 5 BS neurons (n = 111 uEPSPs, blue). Data are presented as cumulative probability plots.

exhibited paired-pulse facilitation (1.39 ± 0.09; n = 7), while L2/3 Pyr-c-AC connections displayed, on average, paired-pulse depression (0.92 ± 0.07; n = 21; P < 0.01; Fig. 6). L2/3 Pyr-BS connections, however, showed both facilitation and depression upon paired-pulse stimulation (1.1 ± 0.2, n = 5, data not shown).

Inhibitory Synaptic Connectivity between L1 Interneurons and L2/3 Pyramidal Neurons

The properties of unitary inhibitory postsynaptic potentials (uIPSPs) recorded from L2/3 pyramidal neurons were found to be dependent on the identity of the presynaptic L1 neuron. In contrast to excitatory connectivity, NGFCs were the most prominent source of inhibition to L2/3 pyramidal neurons, with a connectivity probability of 0.44 (12 connected out 27 connections tested). NGFC-L2/3 Pyr uIPSPs were of long latency, slowly rising, and large amplitude (latency 4.1 ± 0.9 ms, rise time 53.2 ± 10.8 ms, amplitude 0.58 ± 0.1 mV, and half-width 100 ± 19 ms, n = 12). In support of recent observations (Tamas et al. 2003), we observed that a single AP in NGFCs evoked uIPSPs mediated by the activation of both $GABA_A$ and $GABA_B$ receptors ($GABA_A$ receptor antagonist SR 95531, 2 μM and $GABA_B$ receptor antagonist CGP 52432, 10 μM, n = 10, Fig. 7*E,F*). In contrast, the other class of regular-spiking L1 neuron, c-AC cells, generated uIPSPs with a significantly shorter latency (1.8 ± 0.3 ms, P < 0.05), smaller amplitude (0.28 ± 0.04 mV, P < 0.001), and faster kinetics (rise time 6.5 ± 0.5 ms, P < 0.001; half-width 29 ± 8 ms, P < 0.01; n = 4; Supplementary Fig. 5; decay time constant 39.6 ± 6.9 ms [data not shown]). Notably, the probability of connectivity between cAC and L2/3 pyramidal neurons was low (0.06, 4 out of 67 connections tested). Furthermore, c-AC neurons inhibited L2/3 pyramidal neurons through the activation of $GABA_A$ receptors alone as uIPSPs were completely blocked by SR 95531 (2 μM, Fig. 7*B*,7*D*, c-AC: n = 3).

FS neurons are known to act as fast signaling devices in other neuronal circuits (Jonas et al. 2004). Consistent with this role in the superficial cortical layers, FS cells evoked uIPSPs in L2/3 pyramidal neurons with a shorter latency than NGFCs and a faster rise time than other classes of L1 interneurons (uIPSP latency 0.9 ± 0.1 ms, FS vs. NGFC P < 0.01, FS vs. c-AC P = 0.08; rise time 4 ± 0.4 ms, FS vs. NGFC P < 0.001, FS vs. c-AC P <0.05; amplitude 0.27 ± 0.04 mV, FS vs. NGFC P < 0.001, FS vs. c-AC P = 0.77; half-width 27 ± 1 ms, FS vs. NGFC P < 0.001, FS vs. c-AC P = 0.85; n = 3; Supplementary Fig. 5; and decay time constant 31.7 ± 9.5 ms [data not shown]). Moreover, a high connection probability was found between FS and L2/3 pyramidal neurons (0.33, 3/9 connections tested). One chandelier cell was found to be synaptically connected with a layer 2/3 pyramidal neuron and following reconstruction, putative synaptic contacts were found decorating the axon initial segment of the postsynaptic neuron (Supplementary Fig. 7). In line with recent studies (Szabadics et al. 2006; Woodruff et al. 2006, 2009); but see (Glickfeld et al. 2009), we observed that the chandelier cell evoked depolarizing synaptic responses at a membrane potential of –60 mV (Supplementary Fig. 7), in contrast to hyperpolarizing uIPSPs evoked in L2/3 pyramidal neurons by all other classes of L1 interneurons at this membrane potential (see Fig. 7). In common with hyperpolarizing uIPSPs evoked by FS neurons, depolarizing Chandlier-L2/3 Pyr uIPSPs were blocked by the $GABA_A$ receptor antagonist SR 95531 (2 μM, FS: n = 2; Supplementary Fig. 6). Interestingly, none of the BS neurons we recorded were synaptically connected with L2/3 pyramidal neurons (20 connections tested); however, one BS-BS connection confirmed the GABAergic nature of this connection (Supplementary Fig. 8).

Discussion

In this study, we have shown that neocortical L1 neurons can be divided into classes according to the Petilla classification scheme (Ascoli et al. 2008). Hierarchical unsupervised cluster analysis confirmed the division of neurons into 4 groups. L2/3 pyramidal neurons were found to excite L1 neurons in a cell class–specific manner. Surprisingly, we found no excitatory connection between L2/3 pyramidal neurons and NGFCs. In contrast, NGFCs provided strong inhibition of L2/3 pyramidal neurons.

How Many Classes of Interneuron Exist in L1 of the Neocortex?

Previous studies have distinguished, at least, 2 classes of L1 neurons based on electrophysiological and anatomical criteria in brain slices prepared from early postnatal (P7–24) rats (Hestrin and Armstrong 1996; Zhou and Hablitz 1996a; Chu et al. 2003). Local circuit neurons were found to have axonal and dendritic arbors restricted to L1, while deeper layer–projecting neurons possessed descending axons that

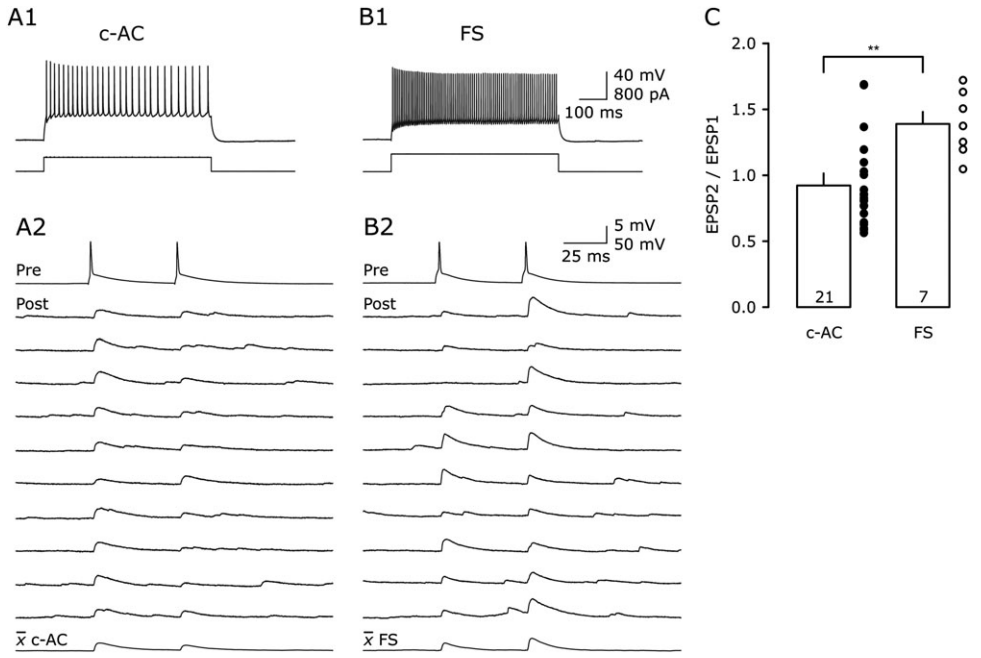

Figure 6. Target-specific short-term plasticity of L2/3 to L1 unitary EPSPs. (*A*1, *B*1) AP firing pattern of a c-AC (left) and an FS neuron (right, upper traces) in response to current injection (lower traces). (*A*2, *B*2) Paired-pulse stimulation in synaptically coupled L2/3 pyramidal–L1 neuron pairs (same neurons as shown in *A*1, *B*1). Top trace (pre, presynaptic L2/3 pyramidal neuron) and 10 consecutive uEPSPs (post, postsynaptic L1 neuron) that were on average (lower trace) depressing in a c-AC and facilitating in an FS neuron. (*C*) Bar plot of the paired-pulse ratio (EPSP2/EPSP1) for L2/3 Pyr-c-AC ($n = 21$) and L2/3 Pyr-FS ($n = 7$) connections (Student's *t*-test, $^{**}P < 0.01$).

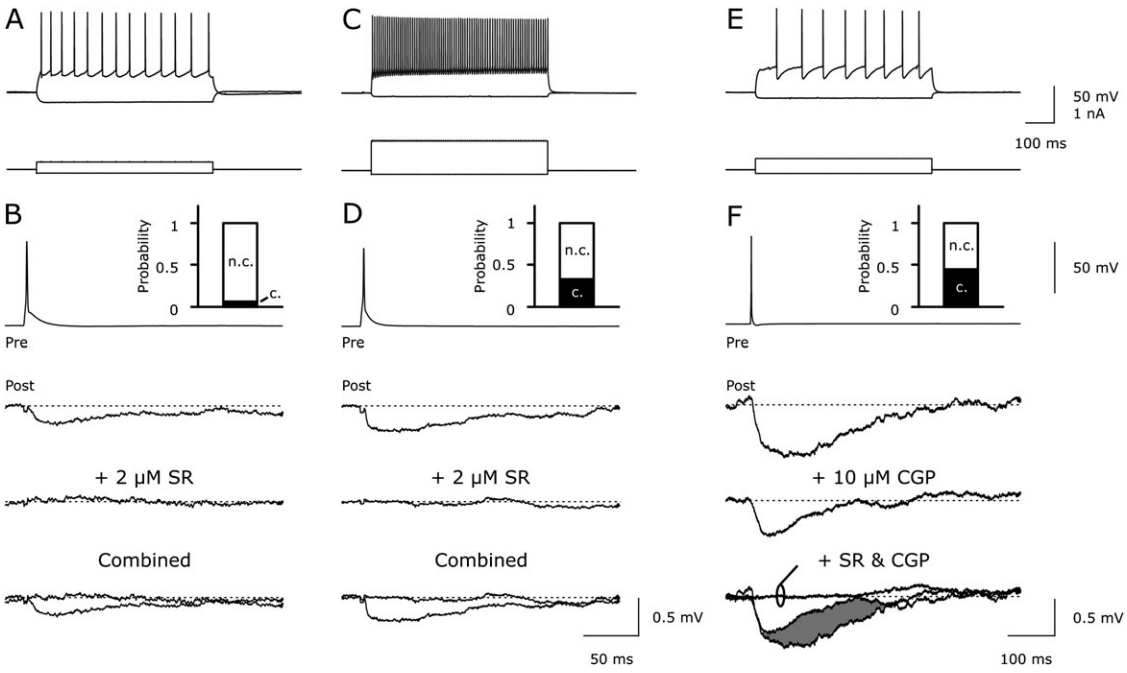

Figure 7. Properties of unitary IPSPs recorded from L2/3 pyramidal neurons evoked by single AP firing in L1 neurons. (*A*) Typical example of the firing pattern of a c-AC neuron (upper trace) in response to current injection (lower traces). (*B*) Average uIPSPs recorded from an L2/3 pyramidal neuron (average of 10 uIPSPs, Post) evoked by AP firing in a c-AC L1 neuron (Pre, same neuron as in A). uIPSPs were blocked by the $GABA_A$ receptor antagonist SR 95531 (2 μM). (*C*) Typical example of the firing pattern of an FS neuron. (*D*) Average uIPSPs in this FS-L2/3 pair were blocked by SR 95531 (2 μM, Pre, same neuron as in *C*). (*E*) Firing pattern of an NGFC. (*F*) Average uIPSPs in an NGFC-L2/3 connection (Pre, same neuron as in E). Note the longer time base. The slow component of the uIPSPs was blocked by the $GABA_B$ receptor antagonist CGP 52432 (10 μM, shaded area in lower panel) and the fast component by SR 95531 (2 μM). *B*, *D*, *F*, Insets show probability of connectivity for each type of L1 neuron.

innervated deeper neocortical layers (Hestrin and Armstrong 1996; Zhou and Hablitz 1996a; Chu et al. 2003). Chu et al. (2003) identified delayed AP firing neurons as NGFCs, that were restricted to L1, while regular firing neurons had axonal arborizations that invaded the deeper layer of the neocortex. In this study, we investigated the properties of L1 neurons maintained in brain slices prepared from P24–36 rats. Over this postnatal age range, the electrophysiological properties of

pyramidal (Zhu 2000; Atkinson and Williams 2009) and interneurons (Doischer et al. 2008) as well as the use-dependent dynamics of unitary excitatory and inhibitory synaptic transmission reach adult levels (Reyes and Sakmann 1999; Angulo et al. 1999; Frick et al. 2007; Feldmeyer and Radnikow 2009). In the mature neocortex, we have identified 4 classes of L1 neurons using unsupervised hierarchical cluster analysis of active and passive electrophysiological properties, a classification scheme supported by morphological analysis.

The role of inhibitory interneurons in neuronal computation is largely determined by the subcellular sites at which inhibitory synaptic contacts are made on pyramidal neurons (Somogyi et al. 1998). For example, classes of cortical interneurons target the axon initial segment, perisomatic regions, or the distal dendrites of pyramidal neurons (Markram et al. 2004; Pouille and Scanziani 2004; Ascoli et al. 2008; Klausberger and Somogyi 2008). Here, we find that the axons of 60% of c-AC neurons and more than 40% of NGFCs were restricted to L1, suggesting that the majority of L1 neurons inhibit pyramidal neurons at the level of the apical dendritic arbor. There are only few reports on FS neurons described in L1 (Foehring et al. 2002). L1 is relatively void of parvalbumin-positive cells, a calcium-binding protein expressed in FS neurons of other neocortical layers (Xu et al. 2010). We have, however, also identified a sparse population (23 of 266) of neurons in L1 with electrophysiological properties of FS neurons that possessed anatomical characteristics of axon or perisomatic-targeting interneurons. We cannot rule out that a small fraction of these neurons have been assigned to the wrong cortical layer because of the proximity of their somata with the L1-L2/3 border. However, based on the finding that only 5 of 271 neurons recorded from layer 1 had properties reminiscent of layer 2/3 pyramidal neurons, we estimate this error to be less than 2%. In support of the view that FS L1 neurons target proximal sites of L2/3 pyramidal neurons, we observed that uIPSPs recorded between FS L1 neurons and L2/3 pyramidal neurons had significantly faster rise times than those generated by dendritic targeting c-AC neurons, presumably because of the influence of dendritic filtering (Miles et al. 1996). As the rise time of uIPSPs also depends on the subunit composition of postsynaptic $GABA_A$ receptors, it is, however, possible that $GABA_A$ receptor composition may influence these findings (Farrant and Nusser 2005).

The minority of L1 neurons possessed axonal projections to deeper layers of the neocortex and were electrophysiologically classified as BS neurons, NGFCs, and chandelier cells. As we failed to observe any inhibitory synaptic input from BS neurons to L2/3 pyramidal neurons, we speculate that such a pathway is sparse and that BS neurons might belong to a group of interneurons which have previously been described to preferentially target other interneurons (Supplementary Fig. 8; (Gulyas et al. 1996; Caputi et al. 2009).

Neuronal Microcircuits in Superficial Layers of the Neocortex

It is widely believed that a canonical microcircuit exists in various cortical areas. In sensory cortices, the flow of information in excitatory neurons of the microcircuit is well described: Thalamocortical projection neurons mainly target spiny stellate cells in L4, which, in turn, innervate L2/3 pyramidal neurons (Feldmeyer et al. 2002; Shepherd and Svoboda 2005). L2/3 pyramidal neurons target neighboring L2/3 (Feldmeyer et al. 2006) and L5 pyramidal neurons (Thomson and Bannister 1998; Schubert et al. 2001; Williams and Atkinson 2007). However, L2/3 and L5 pyramidal neurons also show extensive axonal arborization within L1 (Feldmeyer et al. 2006; Brown and Hestrin 2009). We have found that various interneuron types of L1 receive monosynaptic excitatory input from L2/3 pyramidal neurons. We find the highest connectivity probability in L2/3-FS cell pairs, followed by L2/3-c-AC and L2/3-BS connections. As FS and c-AC interneurons were found to inhibit L2/3 pyramidal neurons, we propose that these cell types may function to provide feedback inhibition.

The use-dependent properties of excitatory synapses have been suggested to determine their role in network function, by shaping the flow of information in neuronal circuits during repetitive AP firing (Abbott and Regehr 2004). Target-specific use-dependent modifications of uEPSPs have been reported in several excitatory synaptic connections in the neocortex (Tsodyks and Markram 1997; Reyes et al. 1998; Markram et al. 1998; Gupta et al. 2000; Rozov et al. 2001; Koester and Johnston 2005; West et al. 2006; Williams and Atkinson 2007). Indeed, the use-dependent properties of uEPSPs evoked from a single presynaptic pyramidal neuron has been found to be dependent upon the identity of the postsynaptic partner (Reyes et al. 1998; Markram et al. 1998; Koester and Johnston 2005). In line with this, we found that the use-dependent properties of excitatory synaptic transmission was dependent upon the postsynaptic target in L1, with L2/3-FS uEPSPs showing paired-pulse facilitation, and L2/3-c-AC depression. Paired recordings from adult rat brain slices have shown that L5 and L6 pyramidal neurons generate facilitating uEPSPs in FS neurons (Angulo et al. 1999; West et al. 2006), whereas synaptic depression has been reported for L2/3-FS synapses in younger animals (P14) (Reyes et al. 1998) and for L4 regular-spiking neurons onto FS neurons (P14–21) (Beierlein et al. 2003). A developmental study, however, has demonstrated that in motor cortices from Wistar rats excitation onto FS undergo marked changes during maturation switching from use-dependent depression at P14–P20 to facilitation at P27–P36 (Angulo et al. 1999).

L1 neurons have been shown to powerfully control the excitability of L2/3 pyramidal neurons in vivo (Shlosberg et al. 2006). However, the functional role of different classes of L1 inhibitory neurons is unknown. Here, we have revealed the existence of 2 inhibitory feedback circuits between L2/3 pyramidal and L1 neurons. We suggest that the contrasting use-dependent properties observed in the excitatory arm of these circuits suggest that c-AC neurons, which target the apical dendritic arbor of L2/3 pyramidal neurons and perisomatically targeting FS neurons will be differentially engaged in a frequency-dependent manner. Both cell types provide feedback inhibition when L2/3 neurons fire APs at low frequencies, however, use-dependent depression at L2/3-c-AC synapses will ensure that dendritic inhibition is dampened during higher frequencies of AP firing. This frequency-dependent routing of feed-back inhibition is in contrast to that found in area CA1 of the hippocampus, where pyramidal to interneuron synapses show use-dependent depression for interneurons that innervate perisomatic sites but facilitation for interneuron that innervate apical dendritic sites of pyramidal neurons (Pouille and Scanziani 2004). In contrast to other classes of L1 neuron, we failed to find excitatory synaptic drive to NGFCs from L2/3

pyramidal neurons. We, however, found that NGFCs generate combined $GABA_A$- and $GABA_B$-mediated inhibitory responses to powerfully inhibit L2/3 pyramidal neurons. Notably, in line with the long latency of NGFCs evoked IPSPs, NGFCs have been shown to release GABA into the extracellular space providing widespread inhibitory input to neighboring neurons (Olah et al. 2009). Because of the large and dense axonal arborization of NGFCs in layer 1, these neurons are ideally positioned in the columnar circuit to control synaptic integration in distal apical dendrites of L2/3 and L5 pyramidal neurons (Waters et al. 2003; Williams 2004; Larkum et al. 2007; Larkum et al. 2009). Indeed, the activation of $GABA_B$ receptors has been shown to powerfully inhibit apical dendritic spike generation in layer 5 pyramidal neurons (Perez-Garci et al. 2006). Similar to hippocampal feed-forward inhibition (Elfant et al. 2008), we suggest that NGFCs may not receive their excitatory input from the columnar circuitry but from long-range intracortical excitatory pathways, conveyed in L1, that synapses with both the apical dendrites of pyramidal neurons (Petreanu et al. 2009) and L1 interneurons (Anderson and Martin 2006). We speculate therefore that NGFCs function to provide powerful feed-forward inhibition of long-range intracortical excitatory input.

Supplementary Material

Supplementary material can be found at: http://www.cercor.oxfordjournals.org/.

Funding

Intramural funding from the Medical Research Council to S.R.W.; EU Marie-Curie Fellowship to C.W.

Notes

We would like to thank the present and previous members of Stephen Williams' laboratory for helpful discussions. We are grateful to Rick Livesey from the Gurdon Institute, Cambridge, UK and the members of the Gurdon Imaging Facility for initial help with confocal images. *Conflict of Interest*: None declared.

References

Abbott LF, Regehr WG. 2004. Synaptic computation. Nature. 431:796–803.

Anderson JC, Martin KA. 2006. Synaptic connection from cortical area V4 to V2 in macaque monkey. J Comp Neurol. 495:709–721.

Angulo MC, Staiger JF, Rossier J, Audinat E. 1999. Developmental synaptic changes increase the range of integrative capabilities of an identified excitatory neocortical connection. J Neurosci. 19:1566–1576.

Ascoli GA, Alonso-Nanclares L, Anderson SA, Barrionuevo G, Benavides-Piccione R, Burkhalter A, Buzsaki G, Cauli B, Defelipe J, Fairen A, et al. 2008. Petilla terminology: nomenclature of features of GABAergic interneurons of the cerebral cortex. Nat Rev Neurosci. 9:557–568.

Atkinson SE, Williams SR. 2009. Postnatal development of dendritic synaptic integration in rat neocortical pyramidal neurons. J Neurophysiol. 102:735–751.

Batista-Brito R, Fishell G. 2009. The developmental integration of cortical interneurons into a functional network. Curr Top Dev Biol. 87:81–118.

Beierlein M, Gibson JR, Connors BW. 2003. Two dynamically distinct inhibitory networks in layer 4 of the neocortex. J Neurophysiol. 90:2987–3000.

Brown SP, Hestrin S. 2009. Intracortical circuits of pyramidal neurons reflect their long-range axonal targets. Nature. 457:1133–1136.

Butt SJ, Cobos I, Golden J, Kessaris N, Pachnis V, Anderson S. 2007. Transcriptional regulation of cortical interneuron development. J Neurosci. 27:11847–11850.

Caputi A, Rozov A, Blatow M, Monyer H. 2009. Two calretinin-positive GABAergic cell types in layer 2/3 of the mouse neocortex provide different forms of inhibition. Cereb Cortex. 19:1345–1359.

Cauli B, Porter JT, Tsuzuki K, Lambolez B, Rossier J, Quenet B, Audinat E. 2000. Classification of fusiform neocortical interneurons based on unsupervised clustering. Proc Natl Acad Sci U S A. 97:6144–6149.

Cauller LJ, Clancy B, Connors BW. 1998. Backward cortical projections to primary somatosensory cortex in rats extend long horizontal axons in layer I. J Comp Neurol. 390:297–310.

Chu Z, Galarreta M, Hestrin S. 2003. Synaptic interactions of late-spiking neocortical neurons in layer 1. J Neurosci. 23:96–102.

Doischer D, Hosp JA, Yanagawa Y, Obata K, Jonas P, Vida I, Bartos M. 2008. Postnatal differentiation of basket cells from slow to fast signaling devices. J Neurosci. 28:12956–12968.

Douglas RJ, Martin KA. 2004. Neuronal circuits of the neocortex. Annu Rev Neurosci. 27:419–451.

Elfant D, Pal BZ, Emptage N, Capogna M. 2008. Specific inhibitory synapses shift the balance from feedforward to feedback inhibition of hippocampal CA1 pyramidal cells. Eur J Neurosci. 27:104–113.

Farrant M, Nusser Z. 2005. Variations on an inhibitory theme: phasic and tonic activation of GABA(A) receptors. Nat Rev Neurosci. 6:215–229.

Feldmeyer D, Lubke J, Sakmann B. 2006. Efficacy and connectivity of intracolumnar pairs of layer 2/3 pyramidal cells in the barrel cortex of juvenile rats. J Physiol. 575:583–602.

Feldmeyer D, Lubke J, Silver RA, Sakmann B. 2002. Synaptic connections between layer 4 spiny neurone-layer 2/3 pyramidal cell pairs in juvenile rat barrel cortex: physiology and anatomy of interlaminar signalling within a cortical column. J Physiol. 538:803–822.

Feldmeyer D, Radnikow G. 2009. Developmental alterations in the functional properties of excitatory neocortical synapses. J Physiol. 587:1889–1896.

Foehring RC, van Brederode JF, Kinney GA, Spain WJ. 2002. Serotonergic modulation of supragranular neurons in rat sensorimotor cortex. J Neurosci. 22:8238–8250.

Frick A, Feldmeyer D, Sakmann B. 2007. Postnatal development of synaptic transmission in local networks of L5A pyramidal neurons in rat somatosensory cortex. J Physiol. 585:103–116.

Glickfeld LL, Roberts JD, Somogyi P, Scanziani M. 2009. Interneurons hyperpolarize pyramidal cells along their entire somatodendritic axis. Nat Neurosci. 12:21–23.

Gulyas AI, Hajos N, Freund TF. 1996. Interneurons containing calretinin are specialized to control other interneurons in the rat hippocampus. J Neurosci. 16:3397–3411.

Gupta A, Wang Y, Markram H. 2000. Organizing principles for a diversity of GABAergic interneurons and synapses in the neocortex. Science. 287:273–278.

Hestrin S, Armstrong WE. 1996. Morphology and physiology of cortical neurons in layer I. J Neurosci. 16:5290–5300.

Howard A, Tamas G, Soltesz I. 2005. Lighting the chandelier: new vistas for axo-axonic cells. Trends Neurosci. 28:310–316.

Jonas P, Bischofberger J, Fricker D, Miles R. 2004. Interneuron diversity series: fast in, fast out–temporal and spatial signal processing in hippocampal interneurons. Trends Neurosci. 27:30–40.

Klausberger T, Somogyi P. 2008. Neuronal diversity and temporal dynamics: the unity of hippocampal circuit operations. Science. 321:53–57.

Koester HJ, Johnston D. 2005. Target cell-dependent normalization of transmitter release at neocortical synapses. Science. 308:863–866.

Larkum ME, Nevian T, Sandler M, Polsky A, Schiller J. 2009. Synaptic integration in tuft dendrites of layer 5 pyramidal neurons: a new unifying principle. Science. 325:756–760.

Larkum ME, Waters J, Sakmann B, Helmchen F. 2007. Dendritic spikes in apical dendrites of neocortical layer 2/3 pyramidal neurons. J Neurosci. 27:8999–9008.

Lubke J, Feldmeyer D. 2007. Excitatory signal flow and connectivity in a cortical column: focus on barrel cortex. Brain Struct Funct. 212:3–17.
Markram H, Toledo-Rodriguez M, Wang Y, Gupta A, Silberberg G, Wu C. 2004. Interneurons of the neocortical inhibitory system. Nat Rev Neurosci. 5:793–807.
Markram H, Wang Y, Tsodyks M. 1998. Differential signaling via the same axon of neocortical pyramidal neurons. Proc Natl Acad Sci U S A. 95:5323–5328.
Miles R, Toth K, Gulyas AI, Hajos N, Freund TF. 1996. Differences between somatic and dendritic inhibition in the hippocampus. Neuron. 16:815–823.
Mitchell BD, Cauller LJ. 2001. Corticocortical and thalamocortical projections to layer I of the frontal neocortex in rats. Brain Res. 921:68–77.
Mountcastle VB. 1997. The columnar organization of the neocortex. Brain. 120(Pt 4):701–722.
Olah S, Fule M, Komlosi G, Varga C, Baldi R, Barzo P, Tamas G. 2009. Regulation of cortical microcircuits by unitary GABA-mediated volume transmission. Nature. 461:1278–1281.
Olah S, Komlosi G, Szabadics J, Varga C, Toth E, Barzo P, Tamas G. 2007. Output of neurogliaform cells to various neuron types in the human and rat cerebral cortex. Front Neural Circuits. 1:4.
Paxinos G, Watson C. 1998. The rat brain in stereotaxic coordinates. 4th ed. San Diego (CA): Academic Press.
Perez-Garci E, Gassmann M, Bettler B, Larkum ME. 2006. The GABAB1b isoform mediates long-lasting inhibition of dendritic Ca2+ spikes in layer 5 somatosensory pyramidal neurons. Neuron. 50:603–616.
Petreanu L, Mao T, Sternson SM, Svoboda K. 2009. The subcellular organization of neocortical excitatory connections. Nature. 457: 1142–1145.
Pouille F, Scanziani M. 2004. Routing of spike series by dynamic circuits in the hippocampus. Nature. 429:717–723.
Prieto JJ, Peterson BA, Winer JA. 1994. Morphology and spatial distribution of GABAergic neurons in cat primary auditory cortex (AI). J Comp Neurol. 344:349–382.
Reyes A, Lujan R, Rozov A, Burnashev N, Somogyi P, Sakmann B. 1998. Target-cell-specific facilitation and depression in neocortical circuits. Nat Neurosci. 1:279–285.
Reyes A, Sakmann B. 1999. Developmental switch in the short-term modification of unitary EPSPs evoked in layer 2/3 and layer 5 pyramidal neurons of rat neocortex. J Neurosci. 19:3827–3835.
Rozov A, Burnashev N, Sakmann B, Neher E. 2001. Transmitter release modulation by intracellular Ca2+ buffers in facilitating and depressing nerve terminals of pyramidal cells in layer 2/3 of the rat neocortex indicates a target cell-specific difference in presynaptic calcium dynamics. J Physiol. 531:807–826.
Rubio-Garrido P, Perez-de-Manzo F, Porrero C, Galazo MJ, Clasca F. 2009. Thalamic input to distal apical dendrites in neocortical layer 1 is massive and highly convergent. Cereb Cortex. 19:2380–2395.
Schubert D, Kotter R, Staiger JF. 2007. Mapping functional connectivity in barrel-related columns reveals layer- and cell type-specific microcircuits. Brain Struct Funct. 212:107–119.
Schubert D, Staiger JF, Cho N, Kotter R, Zilles K, Luhmann HJ. 2001. Layer-specific intracolumnar and transcolumnar functional connectivity of layer V pyramidal cells in rat barrel cortex. J Neurosci. 21:3580–3592.
Shepherd GM, Svoboda K. 2005. Laminar and columnar organization of ascending excitatory projections to layer 2/3 pyramidal neurons in rat barrel cortex. J Neurosci. 25:5670–5679.
Shlosberg D, Amitai Y, Azouz R. 2006. Time-dependent, layer-specific modulation of sensory responses mediated by neocortical layer 1. J Neurophysiol. 96:3170–3182.
Somogyi P. 1977. A specific 'axo-axonal' interneuron in the visual cortex of the rat. Brain Res. 136:345–350.
Somogyi P, Tamas G, Lujan R, Buhl EH. 1998. Salient features of synaptic organisation in the cerebral cortex. Brain Res Brain Res Rev. 26:113–135.
Szabadics J, Tamas G, Soltesz I. 2007. Different transmitter transients underlie presynaptic cell type specificity of GABAA, slow and GABAA, fast. Proc Natl Acad Sci U S A. 104:14831–14836.
Szabadics J, Varga C, Molnar G, Olah S, Barzo P, Tamas G. 2006. Excitatory effect of GABAergic axo-axonic cells in cortical microcircuits. Science. 311:233–235.
Tamas G, Lorincz A, Simon A, Szabadics J. 2003. Identified sources and targets of slow inhibition in the neocortex. Science. 299:1902–1905.
Thomson AM, Bannister AP. 1998. Postsynaptic pyramidal target selection by descending layer III pyramidal axons: dual intracellular recordings and biocytin filling in slices of rat neocortex. Neuroscience. 84:669–683.
Tsodyks MV, Markram H. 1997. The neural code between neocortical pyramidal neurons depends on neurotransmitter release probability. Proc Natl Acad Sci U S A. 94:719–723.
Ward JH. 1963. Hierarchical grouping to optimize an objective function. J Am Stat Assoc. 58:236–244.
Waters J, Larkum M, Sakmann B, Helmchen F. 2003. Supralinear Ca2+ influx into dendritic tufts of layer 2/3 neocortical pyramidal neurons in vitro and in vivo. J Neurosci. 23:8558–8567.
West DC, Mercer A, Kirchhecker S, Morris OT, Thomson AM. 2006. Layer 6 cortico-thalamic pyramidal cells preferentially innervate interneurons and generate facilitating EPSPs. Cereb Cortex. 16:200–211.
Williams SR. 2004. Spatial compartmentalization and functional impact of conductance in pyramidal neurons. Nat Neurosci. 7:961–967.
Williams SR, Atkinson SE. 2007. Pathway-specific use-dependent dynamics of excitatory synaptic transmission in rat intracortical circuits. J Physiol. 585:759–777.
Williams SR, Stuart GJ. 2002. Dependence of EPSP efficacy on synapse location in neocortical pyramidal neurons. Science. 295:1907–1910.
Winer JA, Larue DT. 1989. Populations of GABAergic neurons and axons in layer I of rat auditory cortex. Neuroscience. 33:499–515.
Woodruff AR, Monyer H, Sah P. 2006. GABAergic excitation in the basolateral amygdala. J Neurosci. 26:11881–11887.
Woodruff AR, Xu G, Anderson SA, Yuste R. 2009. Depolarizing effect of neocortical chandelier neurons. Front Neural Circuits. 3:15.
Xu X, Roby KD, Callaway EM. 2010. Immunochemical characterization of inhibitory mouse cortical neurons: three chemically distinct classes of inhibitory cells. J Comp Neurol. 518:389–404.
Zhou FM, Hablitz JJ. 1996a. Layer I neurons of rat neocortex. I. Action potential and repetitive firing properties. J Neurophysiol. 76:651–667.
Zhou FM, Hablitz JJ. 1996b. Postnatal development of membrane properties of layer I neurons in rat neocortex. J Neurosci. 16:1131–1139.
Zhu JJ. 2000. Maturation of layer 5 neocortical pyramidal neurons: amplifying salient layer 1 and layer 4 inputs by Ca2+ action potentials in adult rat tuft dendrites. J Physiol. 526(Pt 3):571–587.
Zhu Y, Zhu JJ. 2004. Rapid arrival and integration of ascending sensory information in layer 1 nonpyramidal neurons and tuft dendrites of layer 5 pyramidal neurons of the neocortex. J Neurosci. 24: 1272–1279.